A virtual reality simulation: classifying stroke patients from healthy controls based on wayfinding features

A. J. Koch

Utrecht University

5483379

Supervisor: dr. Tanja Nijboer

24-08-2021

Abstract

Common cognitive assessment methods often lack ecological validity for assessing complex daily life situations. Virtual reality provides the opportunity to establish controlled and complex daily life-like environments, while capturing the real-time data of patients. In this study 66 stoke patients and 102 healthy controls were subjected to a shopping task inside a Virtual Supermarket (VS) simulation. Movement properties were derived from the coordinate coordinate data that resulted from the VS simulation, and 199 novel way-finding features were extracted. For two separate task types of the VS simulation: a short and a long shopping list, a Logistic Regression model was trained on the optimal subset of wayfinding features. With these models, stroke patients could be distinguished from control subjects, with a performance of an Area Under the Receiver Operating Characteristics (AUROC) of 0.89 with respect to the short list task, and an AUROC of 0.80 for the long list task. The results of this research, suggest a great potential for combining VR simulations with machine learning techniques for innovative cognitive assessment methods, where patients can be exposed to more complex and ecological valid environments.

Keywords: stroke, cognitive assessment, virtual reality, wayfinding, feature extraction, machine learning

1 Introduction

Cognitive impairment often occurs as a consequence of stroke, which has a negative impact on several aspects of daily life, such as social, leisure or work related activities [1]. To assess cognitive impairment in early phase of stroke, universal cognitive screening measures are commonly used. However, these measures have proven to result in poor sensitivity in assessing general cognitive impairment or fail to screen for memory impairments and executive deficits after stroke [2][3]. Moreover, these screening measures often lack ecological validity (i.e. the extent to which these measures generalizes to daily life situations) [4]. Ecological validity of screening measures is needed, because daily life complex situations, such as shopping or travelling, are affected by cognitive impairments [5].

A key example that common screening measures for cognitive impairment have shown to neglect in clinical practice, concerns the *wayfinding* ability of stroke patients [6][7]. Wayfinding in a complex environment represents one of the most fundamental cognitive functions, in which information needs to be integrated from multiple sensory and memory related processes [8]. This complex cognitive construct is pivotal for daily life activities such as moving from one place to the other or doing groceries inside a supermarket. Yet, screening measures assessing wayfinding like mazes and other pencil-paper tasks lack ecological validity for evaluating wayfinding in daily situations.

There is a pressing need for new cognitive screening measures that are ecologically valid and assess cognitive impairment after stroke in more complex environments. The rise of virtual reality (VR) in the recent years, brings a great potential for new cognitive screening measures with high ecological validity [9]. Moreover, VR provides the opportunity to establish a controlled and standardized complex environment. Exposing a patient to that environment with a VR simulation, would not only allow for more ecological valid assessment, but also provides the opportunity to capture *real-time* data of the patient within the virtual environment, in a most detailed fashion.

In this research, the possibility of an innovative cognitive assessment was investigated, based on a wayfinding VR simulation that represents a realistic complex environment of a Dutch supermarket. The aim hereby was twofold: (1) providing a detailed approach of how to pre-process and derive wayfinding properties from complex VR simulations, and (2) trying to capture cognitive impairment caused by stroke by classifying stroke patients from healthy controls, based on wayfinding features derived from the VR data. With the wide availability of VR hardware

and the potential of machine learning classification techniques, there is a great potential for future neuropsychological assessment, where patients can be exposed to more ecological valid environments.

2 Methods: Virtual Simulation

2.1 Participants

For the current study, stroke patients that were either admitted for inpatient rehabilitation or (former) outpatient rehabilitation, were recruited at the Hoogstraat Rehabilitation Center and the University Medical Centre Utrecht. All patients were recruited within a period from June 2016 to July 2019. The inclusion criteria for the study consisted of: (1) being 18 years of age or older; (2) clinical confirmation of stroke with a CT or MRI scan; (3) professional confirmation to be physically and mentally able to take part in the study; (4) reported cognitive complaints in daily life; and (5) no planned clinical assessment within the next three months in case of patients that finished the rehabilitation program. The exclusion criteria consisted of: (1) diagnosis of visuospatial neglect; (2) diagnosis of epilepsy; (3) not being able to use a controller; (4) not being able to execute the task due to communication problems; and (5) confusion and altered alertness problems that prevented the patient from executing the task properly.

The recruitment of healthy controls was done by social media or within the social circles of the staff. The criteria for the healthy controls were the following: (1) being 18 years of age or older; (2) being able to physically use a controller; (3) no history of psychiatric and/or neurological disorders; and (4) no history of epilepsy.

The study was performed in accordance with the Declaration of Helsinki and all participants gave written informed consent. The research protocols were approved by the Medical Research Ethics Committee of the UMC Utrecht (15-761/C, 17-667, 18-210, 18-799 and 19-112).

2.2 Virtual reality simulation

The VR simulation of a *Virtual Supermarket* (VS) was originally developed by Atoms2Bits for commercial purposes. In collaboration with the University Medical Centre Utrecht, the Utrecht University and the Hoogstraat Rehabilitation Centre, the VS was adapted for this study and the potential of an innovative cognitive assessment measure. The VS was designed after a Dutch supermarket and contained 18 shelves with roughly 12.000 products in total, along with different

sections (e.g. dairy and bakery sections) and 8 registers. The floor space was 49.75 by 29.75 meters with a height of 4 meters (Figure 1).

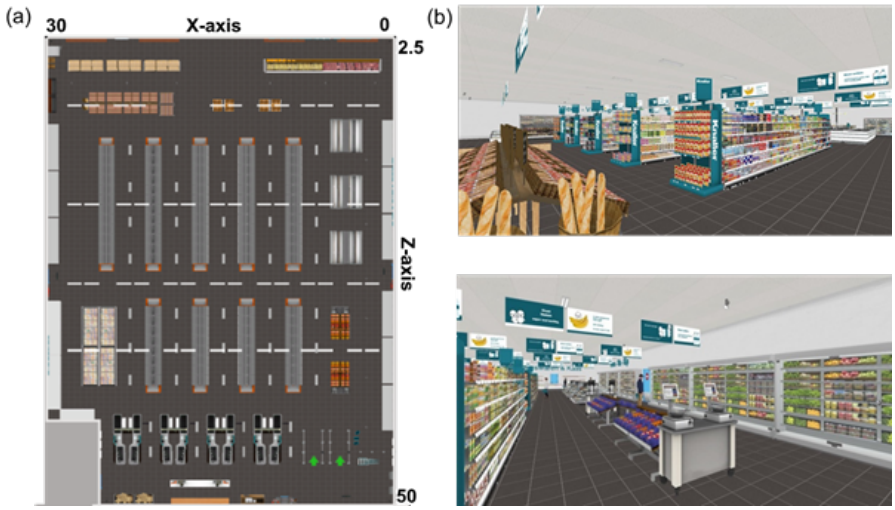

Figure 1: (a) Map of the VR supermarket including the coordinate system in which 1 coordinate represents 1 meter in the virtual environment; (b) screenshots of the VR supermarket.

The VR environment was run on an Intel® Core™ i7-4790K CPU with 16GB of RAM memory and a Geforce® GTX 970 video card, operating on Windows 10 Pro, 64-bit. The virtual environment was displayed on a HTC-Vive head-mounted display, with a 110 degrees diagonal field of view in a resolution of 1080 by 1200 pixels per eye. The participant was able to move through the VS by using two HTC Vive controllers. Each controller was equipped with a button and a trigger. Pulling the triggers resulted in moving through the supermarket. Products inside the VS could be selected by pointing a laser at the product while pressing and holding the button, until the controller vibrated (as an indication that the product was successfully selected). With the use of SteamVR software, the precise location of the head-mounted display and the controllers was tracked by installing two base stations in the corners of the playing field of the participant.

2.3 Task

The task of the participants inside the VS simulation, was to collect products from a shopping list. The list consisted either of *3 products* or *7 products*. The products to be found were described by the name and a picture of the product. Before entering the VS, participants were familiarized

with the VR set up of the head-mounted display and the controllers. They were free to move through a generic virtual environment and when they indicated to be ready to start the task, the experimenter would let them enter the VS. The task started as soon as participants walked through the entry gates of the VS ended when they walked past the cash registers.

As there were two types of tasks, both tasks were separated in two different studies: one study where the participants were to find 3 products (*short list*), and one study where the participants were to find 7 products (*long list*).

2.4 Measurements

Eye movements were recorded using HTC-Vive binocular add-on eye trackers provided by Pupil Labs [10]. The eye trackers included binocular 200 Hz eye tracking cameras with infrared illuminators for each eye. The eye tracking data was configured using Pupil software version 0.9.14.7, developed by Pupil Labs [11]. The 2D coordinate location of the participant during the VS simulation was stored with the same frequency as the eye tracking measures. The software of Pupil Labs also created a log with timestamps of the beginning and the end of the experiment and when products were selected with the laser.

2.5 Data

The eye-tracking and 2D location measures were saved by the software of the VS simulation. The location of the participant within the VS was represented in a 2D manner, with a X-coordinate (depth) and a Z-coordinate (width) expressed in virtual meters. The eye-tracking measures consisted of 3D pupil position coordinates, with an added Y-coordinate (height) measure, for the left and right eye. The 3D coordinates were intersected with the objects inside the VS, combined with the 2D location of the participant inside the VS. All measurements were written to a data file, where each row was represented by one measurement of all outcome measures.

2.6 Pre-processing

The current research focused on the wayfinding ability of the participant during the VS simulation. The first aim was to extract way-finding from the VS simulation outcome measures. Therefore, the raw 2D coordinate location data was first pre-processed in order to come to sensible movement properties, that could not be determined during the actual simulation due to the design of the software.

To talk about the derivation of movement properties from the raw data, the formal notation of the wayfinding data is expressed by the time vector: $T = (t_1, t_2, ..., t_N)$ and its coordinate vectors: $X = (x_1, x_2, ..., x_N)$ and $Z = (z_1, z_2, ..., z_N)$, where N represents the possible number of measurements. Here, T was expressed in seconds, whereas X and Z were expressed in virtual meters. The width of the VS ranging from 0 to 29.75 meters was represented by X, where Z represented the length of the VS ranging from 0 to 49.75 meters.

First, because of the familiarization phase at the beginning of the VS simulation and the closing phase at the end of the simulation, that happened outside the VS, all data files were subsetted for the values of $Z < 46$, marking the entrance and the end of the registers in the VS. This meant that the participant entering the VS was already in motion at the first measurement.

From coordinates X and Z over time T, that represent the walked path of a participant during the VS simulation, three movement properties could be derived: *distance*, *speed* and *direction* [12]. With these properties a total of six new vectors were derived from the original data: X_{diff}, Z_{diff}, D, T_{diff}, S, Dir.

The distance between each measurement for both separate coordinates (X_{diff} and Z_{diff}) was determined by the difference between each coordinate measure (i) and its previous coordinate measure ($i-1$). Resulting in a vector with a length of $N-1$, as for the starting point there is no difference to be determined. From these two vectors, a new vector *Distance (D)* was created that described the distance between point (X_i, Z_i) at measurement (i) and its previous point (X_{i-1}, Z_{i-1}) at the previous measurement ($i-1$), determined by means of Pythagoras with both vectors X_{diff} and Z_{diff}. All distance measures, just as the original coordinate vectors X and Z were expressed in meters.

Just like X_{diff} and Z_{diff}, the time intervals between each measurement were determined in T_{diff}. From D, the *Speed* (S) in each measurement was determined by dividing D by T_{diff}. The speed, expressed by meters per second, was then converted to kilometers per hour.

The *Direction* (Dir) of the movement between each measurement (i) and its previous measurement ($i-1$), was again determined with the use of X_{diff} and Z_{diff}. By taking the arc tangent of X_{diff} and Z_{diff} for all measurements, dividing it by π and multiplying it by 180, results in the direction of movement for each measurement, expressed in degrees ranging from $-180°$ till $180°$. The directions were then mapped into wind directions. The eight compass wind directions, with their corresponding range of directions in degrees, were used to categorize the directions of movement between each measurement. As shown in Table 1, each wind direction was centered around their compass directional degree, with a range of minus $22.5°$ till plus $22.5°$.

With this mapping all possible directions within the range of $-180°$ till $180°$ were captured.

Table 1: All possible wind directions, with their corresponding centers and ranges expressed in degrees.

Wind directions	Direction center	Direction range
N	$0°$	$-22.5° : 22.5°$
NE	$45°$	$22.5° : 67.5°$
E	$90°$	$67.5° : 112.5°$
SE	$135°$	$112.5° : 157.5°$
S	$180°$ ‖ $-180°$	$157.5° : 180°$ ‖ $-180°$: $-157.5°$
SW	$-135°$	$-157.5°; -112.5°$
W	$-90°$	$-112.5° : -67.5°$
NW	$-45°$	$-67.5°; 22.5°$

With the six added movement properties to the original raw coordinate data (X, Z and T), the final pre-processed data set of each participant was expressed by a Multivariate Time Series (MTS) with a total of nine movement properties.

2.6.1 Data exploration, evaluation & transformation

Because the second aim of this study was to extract wayfinding features from the derived movement properties represented in the MTS, and use those features to classify stroke patients from healthy controls, the movement properties derived from the MTS first had to be evaluated. Evaluation was done by plotting the derived movement properties from the raw coordinate data, and evaluating the *mean* and *standard deviation* of each property. Because the direction was expressed as categorical variable, it was evaluated by the *median* direction, but not taken into further evaluation like the numerical properties.

To overcome the irregular sampled data and noise that was present in the raw data, the coordinate data was first transformed by sampling the data with linear interpolation. Sampling the data to a regular spaced grid, allowed for a Fast Fourier Transformation to smooth out the noise in the coordinate data. Because this process of sampling and smoothing is best explained with illustrated examples from the data and the derived movement properties, this process was further elaborated in the results section. All data pre-processing, exploration and transformation was done with the open source programming language of Python 3.7 [13].

3 Results: Virtual Simulation

3.1 Participants

In total, 134 stroke patients participated in the study, due to technical difficulties and aborted experiments, 70 patients could be used for the analysis. Of the stroke patients, 48 did the task with the short list (3 products), and 22 did the task with the long list (7 products). Additionally, 123 healthy control subjects participated in the study and for the same reason as above, only the data of 99 healthy controls could be used for analyses. Of the healthy controls, 28 did the task with the short list, and 71 did the task with the long list. The final demographics are reported in section 5.1 in Table 3, as more patients were excluded later in this study.

3.2 Data exploration

Each raw data file consisted of at least 50.000 rows of data points, where each point indicated one specific measurement of the eye-movement and the 2D location in the VS. Pre-processing the raw data by subsetting for all values of $Z < 46$, resulted in a decline of about 20.000 data points on average. Plotting the coordinates X and Z for all measurements N gives the walked path of a participant over time, as shown in Figure 2a.

On average measurements were done with a time interval of 0.0113 seconds with a standard deviation of 0.0021 seconds. The mean coordinate distances between each measurement were 0.0016 meter ($SD = 0.0021$) for the X-coordinate, 0.0031 meters ($SD = 0.0.0034$) for the Z-coordinate and 0.0039 meter ($SD = 0.0.0036$) for the combined coordinates. The average speed between in measurement consisted of 1.2694 km/h ($SD = 1.1362$) and the median direction was the Norther direction. The results are displayed in Table 2.

Table 2: Mean and standard deviations of the derived movement properties from the VS simulation data, determined for all steps of the sampling and smoothing process.

	T_{diff}		X_{diff}		Z_{diff}		D		S	
	Mean	SD	Mean	SD	Mean	SD	Mean	SD	Mean	SD
Raw	0.0113	0.0021	0.0016	0.0020	0.0031	0.0034	0.0039	0.0036	1.2694	1.1362
Sampled	0.05	0.0005	0.0071	0.0079	0.0139	0.0117	0.0172	0.0120	1.2421	0.8643
Sampled & denoised	0.05	0.0005	0.0051	0.0062	0.0131	0.0111	0.0156	0.0108	1.1238	0.7743
Final	0.3	0.0070	0.0307	0.0350	0.0785	0.0521	0.0934	0.0482	1.1205	0.5782

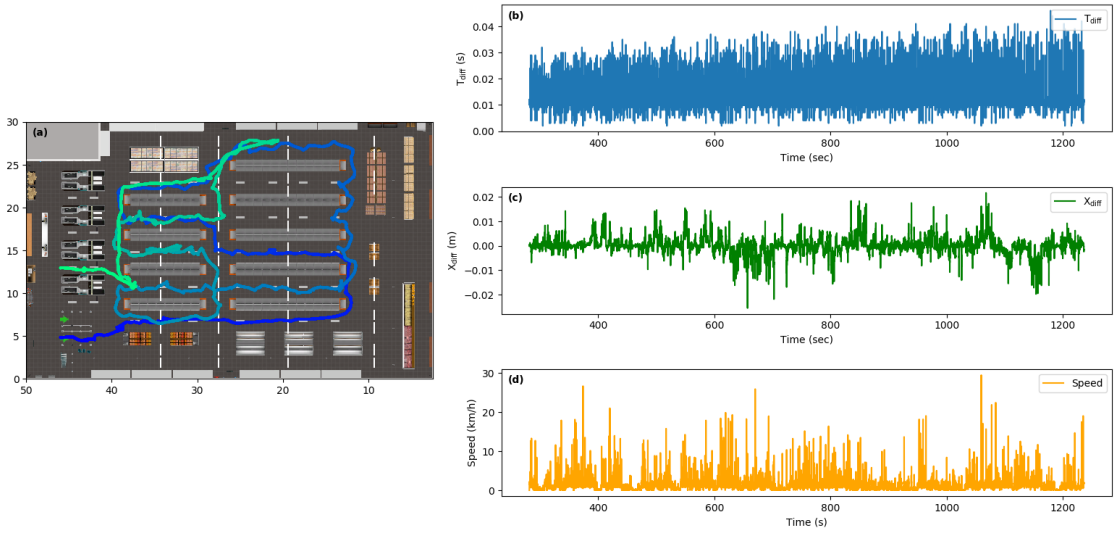

Figure 2: The raw 2D location and movement properties of a participant in the VS. In (a) the walked path of the participant in the VS is plotted over time from blue to green. Here, the Z-coordinates map to the x-axes and the X-coordinates to the y-axes. In (b) the time intervals (T_{diff}) between each measurement are plotted, (c) shows the difference in the X-coordinate between each measurement X_{diff} and in (c) the speed (S) is plotted in km/h. All properties were plotted over time in seconds.

In Figure 2b, 2c and 2d, the movement properties measures T_{diff}, X_{diff} and S are plotted over time. Here it can be seen that all properties displayed some serious irregularities. In Figure 2b the overall trend of time intervals between each measurement lay around 0.011 seconds, however there were many measurements where T_{diff} was way above or below the trend. Irregularities similar to the time intervals were present in all derived movement properties from the raw coordinate data. When determining the speed (S) as described in section 2.6, the speed in particular points resulted to be much higher than the maximum possible speed in the VS of 1.8 km/h, as can be seen in Figure 2d. Here the speed determined from the raw data even reaches a maximum value of over the 25 km/h. To derive sensible wayfinding features from the measured and derived movement properties, the irregularities and outliers from the raw coordinate data first needed to be dealt with.

3.3 Sampling & Noise reduction

First, to overcome the irregular sampled raw data, the coordinate data was sampled to regular time intervals, with linear interpolation. In linear interpolation, a continuous function is defined

that fits all data points of a specific variable. From that continuous function the estimated values of the variable are obtained for the regular time intervals. The raw X- and Z-coordinate data was sampled to create two new coordinate vectors with a regularly spaced grid with time steps of 0.05 seconds. After sampling, the movement properties were again determined from the now regularly spaced 2D coordinate time series data. The results are displayed in the second row of Table 2, and again illustrated in Figure 3 with the movement properties T_{diff}, X_{diff} and S. It can be seen in Figure 3a, that the time interval between each measurement is of a constant value of 0.05 seconds, whereas the in Figure 3b we see that the trend of X_{diff} from the sampled data, is similar to the trend of X_{diff} determined from raw data (Figure 2c). The result of sampling the raw coordinates to a regularly spaced grid with linear interpolation, is illustrated in Figure 3c, where the overall speed contains far less outliers, as compared to the speed derived from the raw data.

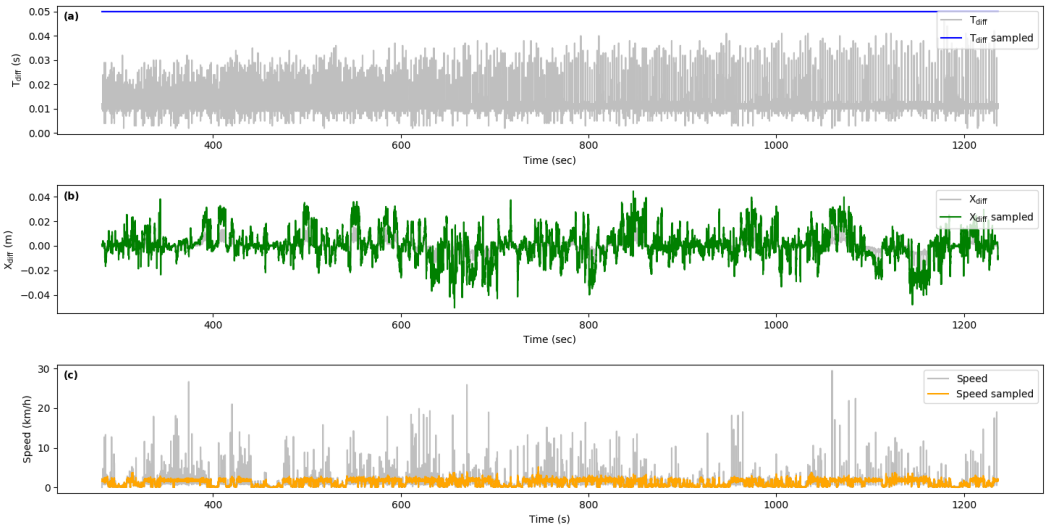

Figure 3: The sampled data movement properties plotted over the raw data movement properties. In (a) it can be seen that the time intervals between each measurement are now of a constant value of 0.05. In (b), X_{diff} shows the same trend as, X_{diff} determined from the raw data, but with greater values, as a result of greater time intervals. In (c) it can be seen that speed contains far less outliers as compared to speed derived from the raw data.

When taking a closer look at X_{diff} and S of the sampled data example in Figure 3, it can be noticed that there were still outliers present in the current sampled data. The noise in the coordinates becomes clear when looking at the raw X_{diff} in Figure 2b and the sampled X_{diff} in

Figure 3b. In both plots, the differences in X between each measurement showed some serious spikes at certain points in time. When looking at the speed in Figure 3c, it shows that the noise in the coordinates is also represented in the speed, despite the now sampled data.

To filter out the noise in the data a *Fast Fourier Transformation* (FFT) was preformed on the sampled X- and Z-coordinates. By applying a FFT on the coordinate data, the data is decomposed into frequencies, that together build up the coordinate signal. Each frequency's contribution to the signal, is expressed through their Power Density Spectrum (PDS) [14]. All frequencies with a PDS higher than 10, were used to reconstruct the coordinate data of X and Z. The application of the FFT on the X- and Z-coordinates is displayed in Figure 4. After the FFT, the movement properties were again determined from the now sampled and smoothed coordinate data, summarized in third row of Table 2. When plotting the X_{diff} and S, the result of this smoothing becomes clear. In Figure 5a and 5b both signals were now much more smoothed compared to the sampled data, and showed no particular outliers throughout time.

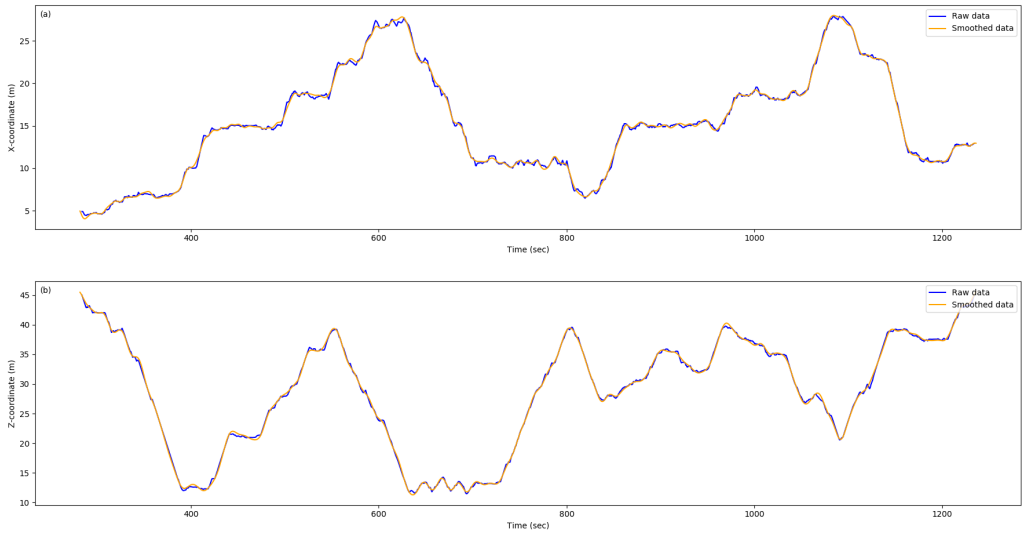

Figure 4: The raw and smoothed coordinate data plotted over time, with the X-coordinate represented in (a) and the Z-coordinate in (b).

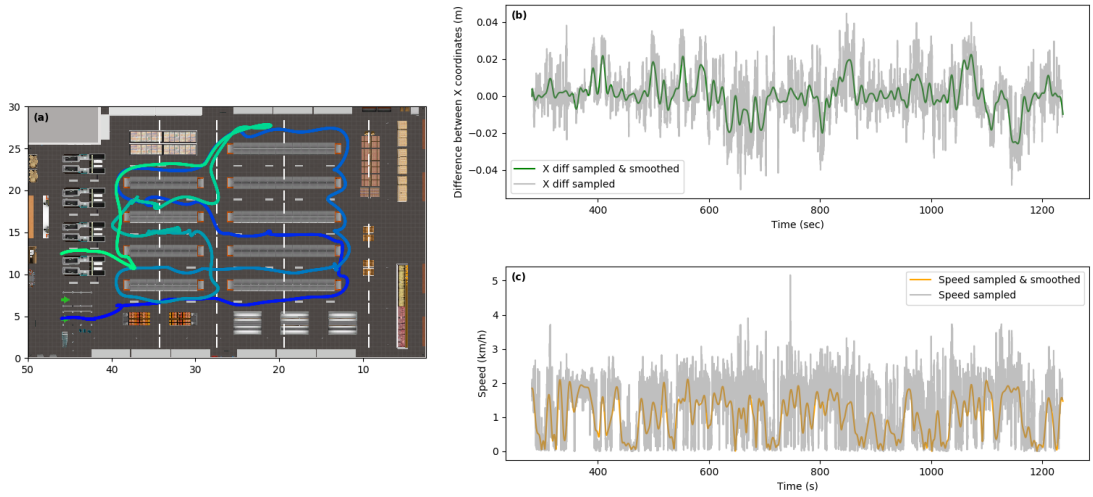

Figure 5: (a) Displays the smoothed and sampled X- and Y-coordinates plotted over time in the VS simulation (from blue to green). In (b) and (c) the movement properties: X_{diff} and the speed S, resulting from the sampled and smoothed coordinate data, are plotted over the properties from sampled data. When comparing both smoothed and sampled properties with just the sampled properties, it shows that both signals were more smoothed compared to the sampled data, and showed no particular outliers throughout time.

In the final stage, for complexity reduction and feature engineering purposes, the data was sampled one more time, to time intervals of 0.3 (SD = *0.007*) seconds. Sampling the data with these time intervals, resulted in a path that showed no differences from a smaller sampling rate, thus still being as detailed as with a sample rate of 0.05 seconds, but reducing the number of measurements by a sixth. The walked path resulting from the sampled and smoothed coordinate data, is plotted in Figure 5a. After the sampling and noise reduction on the raw coordinate data, all movement properties described in section 2.6 were again determined, resulting in the final pre-processed MTS of the movement data of the VS simulation. With the mean and standard variation displayed in the final row of Table 2. The mean distance between each X-coordinate was 0.031 meters (SD = 0.035), the mean distance each Z-coordinate consisted of 0.079 meters (SD = 0.052) and the average distance between each combined coordinate was of a value of 0.093 meters (SD = 0.048). The average speed in each point of the final data was 1.12 km/h with a standard deviation of 0.58.

4 Methods: feature engineering & classification

4.1 Participants

All data that resulted from pre-processing of the VS simulation data of the participants included in Section 3.1, was used to eventually classify stroke patients from healthy controls. For this purpose all healthy controls were labeled 0, where all stroke patients were labeled 1. All participants were checked for outliers on their wayfinding behaviour as further described in Sections 4.3 and 4.4.1.

4.2 Materials

Feature engineering, feature selection and classification was all done in Python 3.7 [13]. Feature selection and classification especially, was done with the Scikit-learn package [15].

4.3 Feature engineering

In order to capture differences in the wayfinding ability of stroke patients and healthy controls, wayfinding features were extracted from the now fully pre-processed MTS. First, basic wayfinding features commonly used to express the performance of one's wayfinding ability, were directly determined from the movement properties: (1) *distance*: the distance (in meters) traveled inside VS simulation, (2) *time*: time spent (in seconds) in the VS simulation and (3) *speed*: the average speed (in km/h) of the participant in the VS simulation [16][17][18].

Secondly, wayfinding behaviour was captured and expressed by *wayfinding events*. We define wayfinding events by particular behaviour of the participant during the VS simulation, characterized by distinctive events. (4) *Stopping behaviour* was extracted from the data in order to capture disorientation, reorientation or product fixation in the VS [19]. Stopping behaviour often indicates that a person is disoriented, as a result stopping behaviour is performed to find one's way [20]. Stopping behaviour was defined by a participant by moving no less than 0.36 km/h, for a minimal amount of time of 3 seconds. The threshold of 0.36 km/h was chosen, because a complete standstill inside the VS was not possible due the VR setup. Thereby, in a stopping motion the subject is likely to orientate by moving around, causing minor movements during the stopping motion. As an addition to stopping behaviour, (5) *slowing-* and (6) *speeding behaviour* were taken into account as well. As slowing behaviour might also indicate orientation behaviour or uncertainty in movement by the participant, whereas speeding behaviour would indicate a

more confident movement through the VS. Slowing behaviour was defined by consecutive speed measurements within a range of 0.36 km/h up till 0.72 km/h for at least three seconds, where speeding behaviour was defined by a speed of at least 1.8 km/h for a minimal amount of three seconds. All three types of wayfinding events are illustrated in Figure 6.

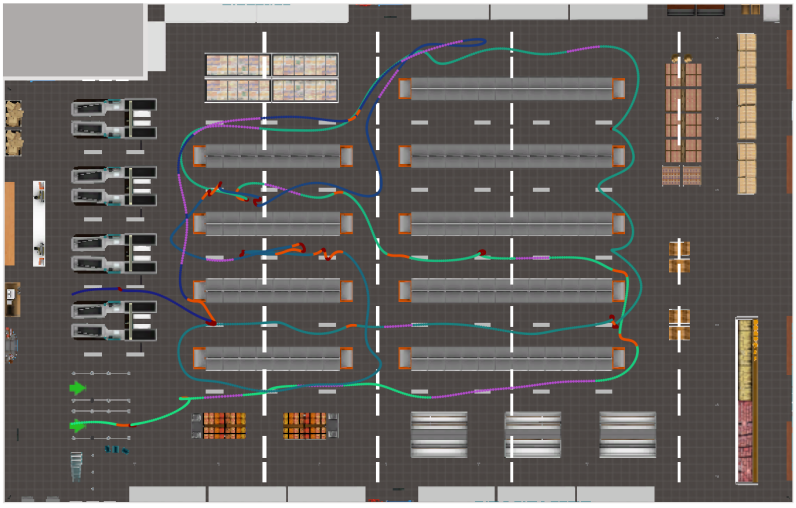

Figure 6: Wayfinding events of: stopping behaviour (red), slowing behaviour (orange) and speeding behaviour (purple). All events are plotted over the route travelled in the VS, plotted over time (from green to blue).

During wayfinding, people are inclined to make as few changes in direction as possible and prefer straight routes [21][22]. Therefore, (7) *direction changes* were captured, expressed by the number of times the participant changed direction, from one direction to the other inside the VS simulation. To further analyze the directional behaviour of the participants during the VS simulation, a distinction was made between (8) *straight walking behaviour* and *non-straight walking behaviour*. Straight walking behaviour was defined by consecutive measurement of the same direction, for a minimal amount of time of 3 seconds and a minimal distance of 0.75 meters. All consecutive measurements that did not met these criteria and fell in between two straight walking behaviours, were defined as non-straights walking behaviours. The non-straights walking behaviour (ns) was further divided 2 types of events: *turns* and *continuations* [23][24]. A ns was defined as a turn, when the wind direction of the straight walking behaviour before the ns was at least 90 degrees (two wind directions) apart from the wind direction of the straight walking

behaviour after the ns. Within the event of a turn, again two distinctions were made: a (9) *smooth turn* and a (10) *complex turn*. A smooth turn consisted of no more than three consecutive wind directions, while a complex turn was defined as a turn that contained more than three wind directions. The event of a continuation was defined by when the the wind direction of the straight walking behaviour before the ns was the same or just one wind direction apart from the wind direction of the straight walking behaviour after the ns. Here again two distinctions were made between continuations: (11) *smooth continuations* and (12) *complex continuations*, marked by the same criteria of the distinction between turns. The four sub events of non-straight walking behaviour are displayed in Figure 7.

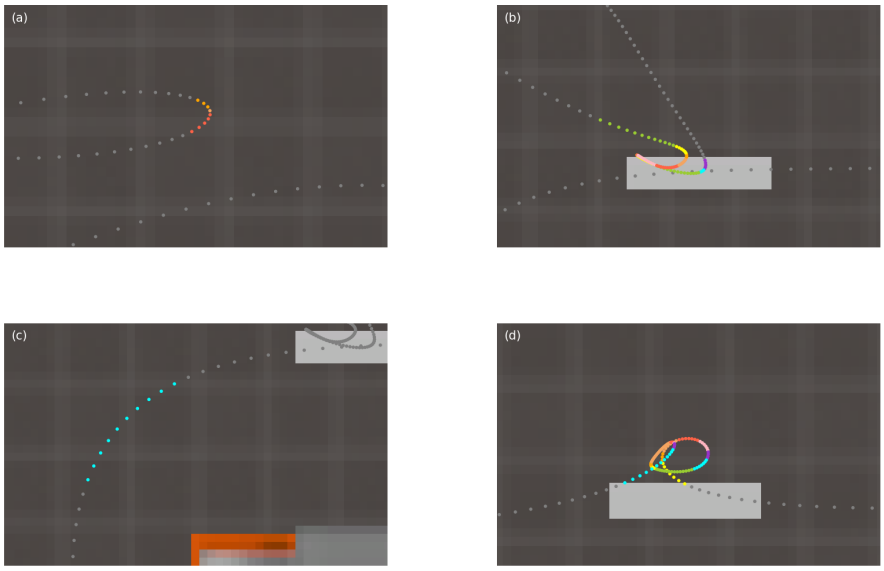

Figure 7: The four types of *non-straight* behaviour: smooth turn (a), complex turn (b), smooth continuation (c), complex continuation (d). All non-straights are depicted in color, where each different color stands for a different wind direction.

Efficiency of ones path through the VS simulation, could also be evaluated by (13) *path intersections* [25]. Path intersections were defined by evaluating the path of the participant over time. For each measurement a path segment was defined between that measurement i and its previous measurement $i-1$. For each segment (in consecutive order) the segment was checked for intersecting with the path consisting of all previous path segments.

In the end, in order to come to sensible and informative feature measures, 8 wayfinding events (4-6, 8-12) were expressed in four different measures: *number of occurrences*, *number of*

occurrences per meter, *total duration of occurrences*, *average duration of occurrences*. Direction changes (4) and path intersections (13) were expressed in two measures: *number of occurrences*, *number of occurrences per meter*. Resulting in a total of 39 wayfinding features.

The VS was divided into predefined sections that all corresponded with a type of aisle, where each type of aisle was believed to have a potentially different wayfinding behaviour. First, two types of aisle were defined: *vertical aisles*: aisles with no products shelves, and *horizontal aisles*: aisles with product shelves. Visual and directional cues in a virtual environment, contribute to the orientation of the subject [26]. As the vertical aisles only contained orientational and directional cues (e.g. a sign pointing towards the canned goods aisle), more orientational wayfinding behaviour was expected. Horizontal aisles were further divided into two sub types: *target aisles*: aisles that contained target products from the shopping list, and *non-target aisles*: aisles that contained no target products. Here, different wayfinding behaviour was expected as well, as target aisles might trigger more search behaviour, whereas non-target aisles could be quickly skipped through. In an attempt to capture the efficiency of the route of the participant during the VS simulation, *the number of aisles revisits* were captured and summarized for all four aisle sub types. For every aisle sub type: all 40 wayfinding features described in this section were determined. Resulting in a subset of 160 features, in total coming to 199 different wayfinding features (Appendix A).

4.4 Feature selection

With the total set of wayfinding features, dimensionality reduction of the features was needed to avoid overfitting of the classifying models. Training a classifying model on a large number of features, results in the model becoming increasingly dependent on the data, and as a result the model becomes overfitted. Moreover, the less features a model is trained on, the less complex it becomes by making less assumptions based on the data. Therefore, feature selection was performed to reduce the dimensionality of the features, creating more transparent models without overfitting. Feature selection was done separately for both the *short list* and the *long list* datasets.

4.4.1 Anomaly detection & Scaling

First in both the data sets, all anomalies (i.e. participants that performed abnormal wayfinding behaviour within the VS simulation) were detected and isolated by means of the *Isolation Forest* method [27]. This method allowed for high anomaly detection performance, over the high

dimensional feature data set. After the removal of the anomalies, all feature were standardized by removing the mean and scaling to unit variance.

4.4.2 Feature Importance

From the 211 wayfinding features, the most contributing features regarding to the label of the participants (i.e. being a healthy control or a stroke patient), were determined and selected for both separate data sets. This was done by a Recursive Feature Elimination (RFE) with cross validation. With RFE, a model is trained on all features that determines the importance of each feature within that model. The least important features are removed, and then the process is repeated recursively with the new subset of features. Performing RFE with cross validations allows to find the optimal number of features, by scoring different feature subsets and select the best scoring collection of features. For both data sets, two separate subsets of optimal features were determined for the final model. The model used for RFE was the same model eventually used for the classification task: a *logistic regression model*. To prevent the model from overfitting and to deal with the high dimensionality of the wayfinding features, the model was run with a L1 regularization. As a final step, the optimal subset of wayfinding features was checked for multicollinearity by determination of the Variance Inflation Factor (VIF) for all features. Multicollinearity is a problem for the final logistic regression model, since high multicollinearity makes it more difficult to estimate the relationship between each of the wayfinding variables and the label. Therefore, all features with a VIF higher than 2.5 were removed from the subset [28].

4.5 Classification

Classifying stroke patients from healthy controls based on the optimal subset of wayfinding features, was done with a *logistic regression* model. Because the dimensionality reduction of the features by RFE, no regularization by a L1 penalty was needed anymore. The classifying model was trained and tested using a stratified cross validation. Stratification was needed, to account for the class imbalance in both datasets. With stratified cross validation the same class distribution as the original dataset is maintained throughout each fold. Because of the imbalanced data, the performance of both models was expressed by the Area Under the Receiver Operating Characteristics (AUROC) curve. The cross validation was repeated a 100 times, and the mean and standard deviation of the AUROC curve was taken as a final performance measure.

5 Results: feature engineering & classification

5.1 Participants

With the anomaly detection, a total of 10 instances were filtered from the short list data set, where 10 instances were filtered from the long list data set. All anomalies are depicted in Figure 8, where the decision scores, determined by the isolation forest method, are plotted for all instances. After the anomaly removal the short list data set consisted of 31 healthy controls and 48 stroke patients. The long list data set consisted of 71 healthy controls and 18 stroke patients. Summarized in Table 3.

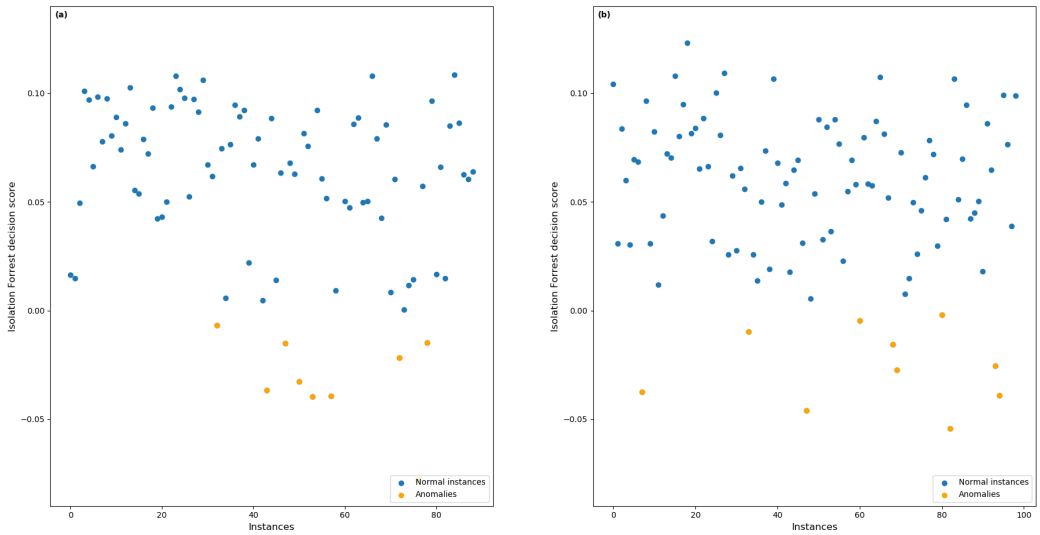

Figure 8: All detected and isolated anomalies by the Isolation Forest method, (a) displaying the decision scores of the participants from the short data set, (b) displaying the decision scores of the participants from the long data set

Table 3: Demographics of all participants, with additional medical characteristics of the stroke patients.

	Stroke (n=66)	Control (n=102)
Mean age in years (*SD*)	54.73 (12.3)	44.54 (14.89)
Male %	58	44
Education Low	12.2	1
Average	25.8	7.9
High	59.1	91.1
3 products %	72.7	30.7
7 products %	27.3	69.3
Mean days post-stroke onset (*SD*)	619.3 (1118.32)	-
Lesion side %		
Left	45.5	-
Right	34.8	-
Both	9.1	-
Unknown	10.6	-
Stroke type %		
Ischemic	57.6	-
Haemorrhage	19.7	-
Subarachnoid Haemorrhage	13.6	-
Subdural Hematoma	3	-
Sinus Thrombosis	1.5	-
Unknown	4.5	-
Stroke history %		
First	83.3	-
Recurrent	12.1	-
Unknown	4.5	-

5.2 Feature selection: short list task

The optimal set of wayfinding features for the short list task, determined by the cross validated RFE with 20 repeats, consisted the following 13 features: (1) *Target revisits*, (2) *Average speed (nontarget)*, (3) *Stopping behaviour (average time (horizontal))*, (4) *Speeding behaviour (occurrences / meter (vertical))*, (5) *Speeding behaviour (occurrences / meter (nontarget))*, (6) *Straight walking behaviour (vertical)*, (7) *Direction changes (occurrences / meter)*, (8) *Straight walking behaviour (vertical)*, (9) *Smooth turns (total occurrences (vertical))*, (10) *Complex turns (total occurrences (vertical))*, (11) *Complex turns (occurrences / meter (target))*, (12) *Smooth continuations (total occurrences (horizontal))*, and (13) *Complex continuations (occurrences / meter (vertical))*. The feature *Straight walking behaviour (vertical)*, resulted in a VIF of 3.28 and thus was removed from the subset of wayfinding features. In Figure 9 all distributions of the final optimal set of wayfinding features for the short list task are plotted.

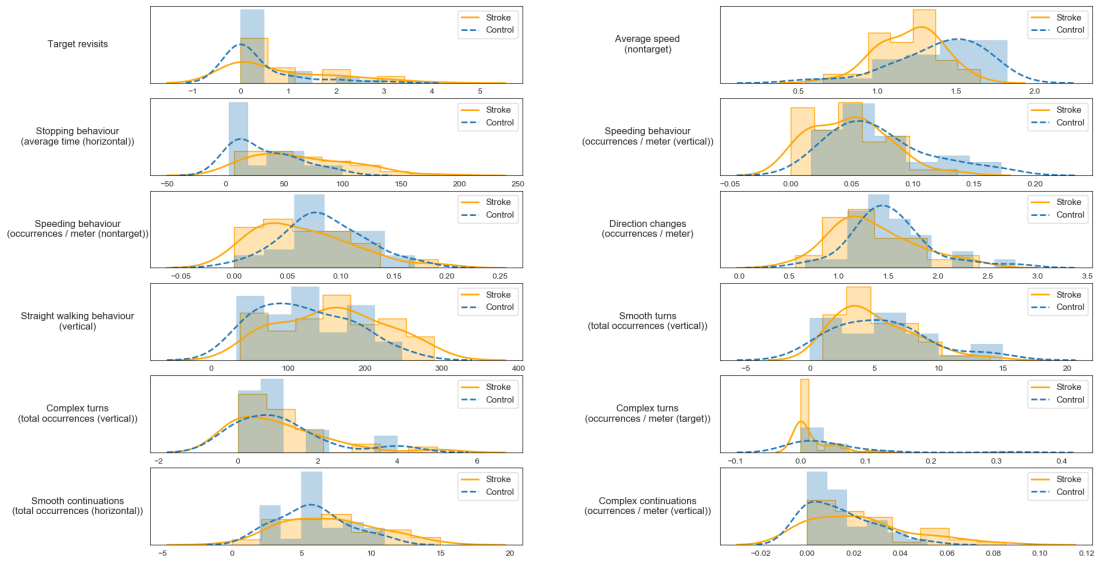

Figure 9: Distribution of optimal feature sets of the short list shopping list. With the distributions of the healthy controls in blue, and distributions of the stroke patients in yellow.

5.3 Feature selection: long list task

The optimal set of wayfinding features for the long list task consisted of: (1) *Slowing behaviour (total time)*, (2) *Smooth turns (total time)*, (3) *Total time (horizontal)*, (4) *Stopping behaviour (vertical)*, and (5) *Complex turns (occurrences / meter (target))*. No features in this subset

showed any sign of multicollinearity. The distribution of each wayfinding feature from the optimal subset, are plotted in Figure 10.

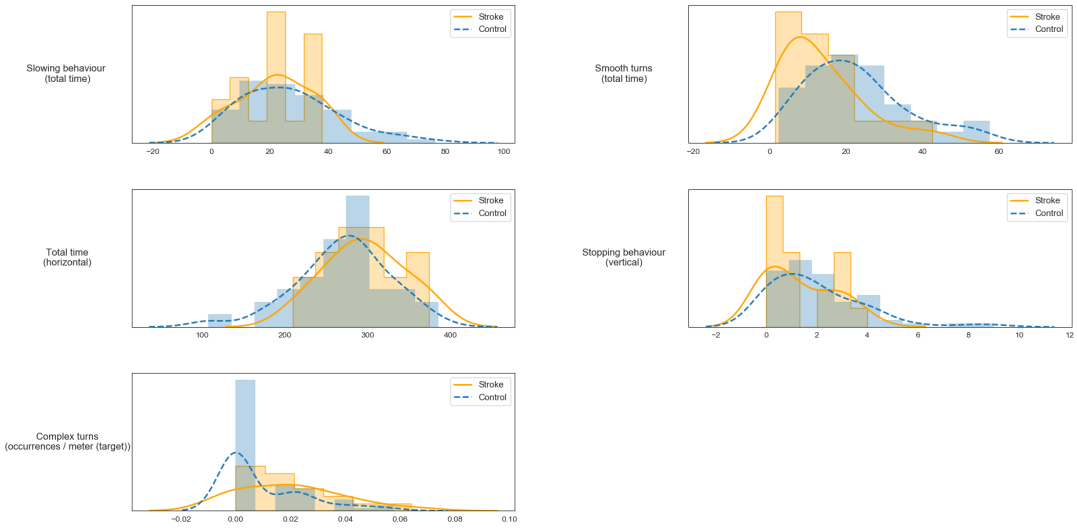

Figure 10: Distribution of optimal feature sets of the short long shopping list. With the distributions of the healthy controls in blue, and distributions of the stroke patients in yellow.

5.4 Classification: short list task

A 100 times repeated stratified cross validation of a Logistic Regression model with the optimal subset of wayfinding features based on the short list data set, resulted in a mean AUROC of 0.89 (SD= 0.05) when classifying stroke patients from healthy controls. The mean AUROC with its standard deviation is displayed in Figure 11a. The feature with the highest coefficient importance concerned the feature of: the *average speed* in the nontarget aisles (Figure 11b).

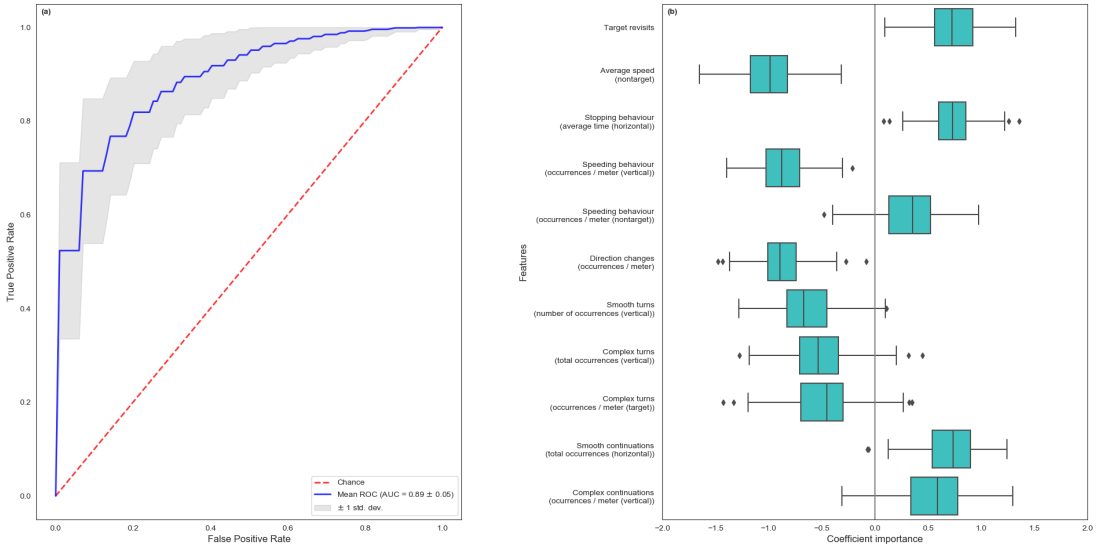

Figure 11: The performance of the short list Logistic Regression model based on the optimal subset of wayfinding features. In (a) the performance of the model is illustrated by plotting the True Positive Rate (y-axes) over the False Positive Rates (x-axes). The red line indicates the performance of a baseline model that would classify the labels by chance. In (b) a box plot of the coefficient importance of all features used in the model is displayed.

5.5 Classification: long list task

For the long list data set and the optimal subset of wayfinding, the Logistic Regression model classified stroke patients from healthy controls wit a mean performance of 0.80 (SD= 0.06). From Figure 12b, it can be seen that the most important feature that resulted from this model, was the total time spent on *smooth turns*.

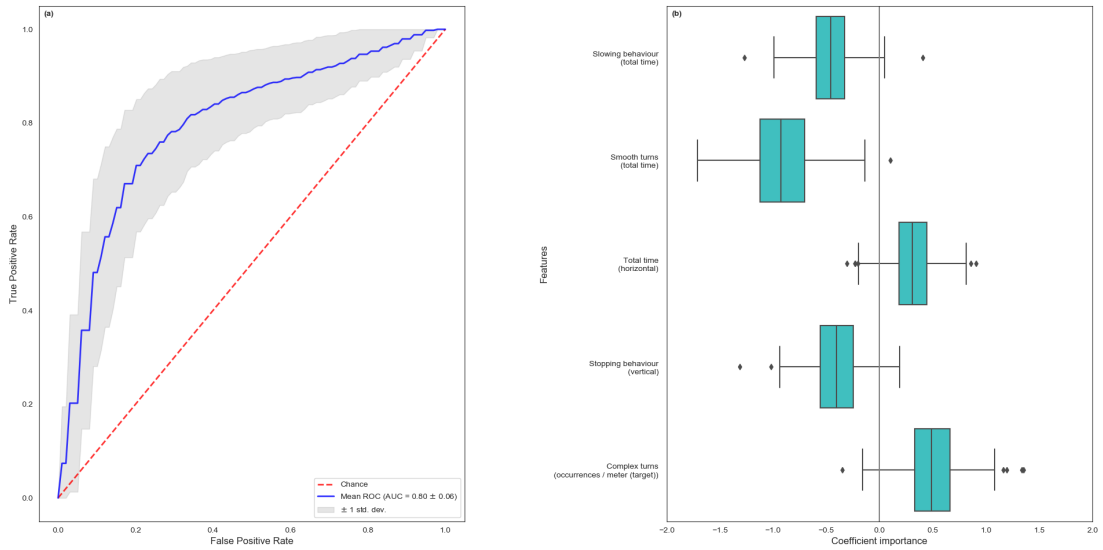

Figure 12: The performance of the long list Logistic Regression model based on the optimal subset of wayfinding features. In (a) the the performance of the model is illustrated by plotting the True Positive Rate (y-axes) over the False Positive Rates (x-axes). The red line indicates the performance of a baseline model that would classify the labels by chance. In (b) a box plot of the coefficient importance of all features used in the model is displayed

6 Discussion

The aim of this study was two fold: (1) to extract novel wayfinding features from derived movement properties of a virtual supermarket simulation, and (2) trying to capture cognitive impairment caused by stroke by classifying stroke patients from healthy controls, based on the extracted wayfinding features. First the coordinate data resulting from the VS simulation, was sampled and smoothed in order to derive sensible movement proprieties from the data. From the derived movement properties, 199 wayfinding features were extracted. For two separate task types of the VS simulation: a short and a long shopping list, a optimal subset of features was determined. With each subset of wayfinding features a model was trained to distinguish stroke patients from healthy controls, resulting in an accuracy of 0.89 for the short list model, and a 0.80 accuracy for the long list model.

To overcome noise in the raw coordinate data that resulted from the VS simulation, first sampling with interpolation was applied. Sampling was needed to create a regular sized grid of time intervals, in order to smooth our data with a Fast Fourier Transformation. Deriving

movement properties from the sampled and smoothed data resulted in sensible measures, with no particular outliers. An interesting question to ask here, is why the noise was present in the raw data in the first place. An explanation for this can be found in the VR setup that resulted in the measurements of the coordinates during the VS simulation. Due to the software design, the virtual location of a participant in the VS, was not only determined by the controller, but also influenced by the head mounted display that the participant wore during the VS simulation. Therefore, head movements during the VS simulation, were also recorded and integrated with the coordinate measurements. Although head movements consist minor movements, the speed of these movements could possibly have caused relatively big changes in the virtual position between each measurement, represented for example by the spikes in the derived speed from the raw data in Figure 2d. Interesting to note was that sampling the raw data already resulted in a decline of outliers. This could be explained by the notion that linear interpolation of irregular measurements onto a regular spaced grid causes an additional bias towards low frequencies in power spectral density (PSD) estimation [29]. Assuming that the low frequencies are represented by the controller movements, this could explain why the noise represented by the head movements was partially suppressed by sampling with linear interpolation. This notion was further supported by the Fast Fourier Transformation on the coordinate data, which did not result in a clear identification of the noise components in our sampled data, as the reconstructed data by linear interpolation was probably more biased towards the controller movements. Other sampling techniques like a Gaussian kernel-based estimator might have been better suited to reconstruct the coordinate data to regular time intervals, although bias properties are still persistent in these methods as well [30]. In the end, the easiest solution would have been to separately measure the controller and the head movements during the VS simulation from the start.

In line with expectation of the research of [6], the current study suggest that based on the wayfinding features from the VS simulation, there is a difference in the wayfinding ability between stroke patients and healthy controls. Studies also show that patients with mild cognitive impairments (MCI) often show spatial and orientational navigation impairments, and that spatial navigation impairments even can be used as a marker for agnostic MCI [7][31]. The results of the current study might suggest the same for cognitive impairments and the wayfinding ability of stroke patients, as based on the extracted wayfinding features, stoke patients could be distinguished from the healthy controls. As it is supported by previous studies that virtual environments can be characterized by their enhanced ecological validity [9][32]. This study demonstrates the great potential for innovative cognitive assessment methods, by assessing cog-

nitive impairment based on identified markers, derived form complex daily-life VR simulations.

In this study, two subsets of optimal wayfinding features were determined regarding to classifying stroke patients from healthy controls for both task types of the VS simulation. The most important wayfinding feature of the short list model was found to be the average speed of the participant in the non-target aisles. In the distribution of Figure 9, it is evident that control subjects move faster through the non-target aisles as compared to stroke patients. This might indicate that stroke patients are less efficient when moving through the virtual environment, as stroke patients might need more time to process their surroundings due to slower search strategies [33]. The most important feature in the long list model was the total time spent on smooth turning behaviour. The study of [34] suggest that during the performance of a turn, motion performance and gaze coordination are affected by cognitive impairments in stroke patients. Based on the distribution plot in Figure 12, this might indicate why stroke patients perform less smooth turns than healthy controls. Since while performing a turn, the movement ability of the stroke patients is affected and therefore, less smooth turns could be expected. This notion could also be supported by the only feature that was present within the both subsets of optimal wayfinding features: the average number of complex turns per meter in the target aisles. Complex turns consisted of a change in direction that was characterized by a multiple direction changes within that turn, as illustrated in Figure 7b. In the target aisles more coordinated gaze behaviour is required to search for the target product, in an event of a turn this might result in even less efficient moving of the stroke patient, causing a complex turn. Interesting to see is that when we look at the coefficient importance of this feature in both task type models in Figure 11b and 12b, we note that the coefficient importance of the feature is of a negative coefficient in the short list data set, but of a positive coefficient in the long list dataset. This could be explained by the fact that the coefficient importance illustrates the *conditional* importance of the features, i.e. the coefficient importance is only of that specific value because of the presence of the other features [35]. To gain a more complete picture of how these wayfinding features are represented among the stroke populations as compared to healthy controls, more explanatory research is necessary with respect to the interpretation of these features.

With regard to the current study there were some limitations that have to be mentioned. The first limitation of this research concerned the small sample sizes of the two task types of the VS simulation. In machine learning a large sample size is needed to provide enough power for the models. Especially when dealing with complex and nonlinear data in classification problems, large sample sizes are needed to capture the relation between the variables and the

label. However, by using a fairly simple and interpretable model like the Logistic Regression combined with stratified cross validation, a good performance of the model could still be achieved. The relatively a low standard deviation of the mean performance in both models, and the notion that *both* models in this research performed well, indicates the potential of capturing wayfinding from a VR simulation as an innovative cognitive assessment method. Another limitation of the current study that should be noted, was the reduction of participants that ended up in the final models. Due to technical difficulties or aborted VS simulations, 64 stroke patients and 24 control subjects had to be excluded from the analysis. It is remarkably that almost a three quarters of the excluded subjects consisted of stroke patients. Although it is argued by [36] that cognitive assessment with VR is feasible, further research should investigate on how to reduce the numbers of exclusion in order to create feasible and valid innovative cognitive assessment methods. Besides exclusion because technical difficulties or aborted simulations, an additional 14 stroke patients and 6 control subjects were removed as anomalies. Given the small sample size in both task types, this might be problematic. Future research should be done in regard to analyzing wayfinding with this type of VR setup, and how the wayfinding ability of participants might be influenced in a virtual environment or what causes these anomaly behaviours.

With the eye on future research, the VS simulation still offers many more potential for cognitive assessment. In this study, only the coordinate data of the VS simulation was used to derive wayfinding features and to classify stroke patients from healthy controls. Classification with wayfinding features could also be combined with eye-tracking measures, to capture the visual search and wayfinding behaviour of the participant during the VS. The current study classifies stroke patients from healthy controls, but future research could also provide more details on the relation of wayfinding features with multiple cognitive domains. This research provides the a next step in more advanced cognitive assessment, as machine learning could be applied to gain more insight in the relation between the wayfinding features and outcome measures of existing cognitive screening test on several cognitive domains.

Conclusion

This study demonstrates the potential of innovative cognitive assessment methods by using a virtual reality simulation. Based on wayfinding features derived from the simulation of a virtual supermarket, stroke patients be could classified from healthy controls with a high performance. This promising result is a serious step towards more ecological valid assessment of cognitive impairments experienced in complex daily life situations.

Acknowledgements

I'd like to thank Alex Hoogerbrugge for providing the scripts and data pipelines from the eye-tracking toolbox designed for the virtual supermarket, that were of huge help for me to start this project. I thank Malouke Visser for all her help in coming up with sensible wayfinding features, and providing clarity around the study protocols. Last but not certainly least, I want to thank dr. Tanja Nijboer for all her supervision and her flexibility during this whole project.

References

[1] E. Shevil and M. Finlayson, "Perceptions of persons with multiple sclerosis on cognitive changes and their impact on daily life," *Disability and Rehabilitation*, vol. 28, no. 12, pp. 779–788, 2006.

[2] H. Blake, M. McKinney, K. Treece, E. Lee, and N. B. Lincoln, "An evaluation of screening measures for cognitive impairment after stroke," *Age and ageing*, vol. 31, no. 6, pp. 451–456, 2002.

[3] G. Nys, M. Van Zandvoort, P. De Kort, H. Van der Worp, B. Jansen, A. Algra, E. De Haan, and L. Kappelle, "The prognostic value of domain-specific cognitive abilities in acute first-ever stroke," *Neurology*, vol. 64, no. 5, pp. 821–827, 2005.

[4] D. R. Dawson and T. D. Marcotte, "Special issue on ecological validity and cognitive assessment," 2017.

[5] R. Kizony, T. Demayo-Dayan, G. Sinoff, and N. Josman, "Validation of the executive function route-finding task (efrt) in people with mild cognitive impairment," *OTJR: occupation, participation and health*, vol. 31, no. 1_suppl, pp. S47–S52, 2011.

[6] I. J. van der Ham, N. Kant, A. Postma, and J. Visser-Meily, "Is navigation ability a problem in mild stroke patients? insights from self-reported navigation measures," *Journal of rehabilitation medicine*, vol. 45, no. 5, pp. 429–433, 2013.

[7] G. Coughlan, J. Laczó, J. Hort, A.-M. Minihane, and M. Hornberger, "Spatial navigation deficits—overlooked cognitive marker for preclinical alzheimer disease?" *Nature Reviews Neurology*, vol. 14, no. 8, pp. 496–506, 2018.

[8] T. Wolbers and M. Hegarty, "What determines our navigational abilities?" *Trends in cognitive sciences*, vol. 14, no. 3, pp. 138–146, 2010.

[9] T. D. Parsons, "Virtual reality for enhanced ecological validity and experimental control in the clinical, affective and social neurosciences," *Frontiers in human neuroscience*, vol. 9, p. 660, 2015.

[10] "Pupil labs htc vive binocular add-on, author=Pupil Labs, journal=https:pupil-labs.com, year=2020."

[11] M. Kassner, W. Patera, and A. Bulling, "Pupil: an open source platform for pervasive eye tracking and mobile gaze-based interaction," in *Proceedings of the 2014 ACM international joint conference on pervasive and ubiquitous computing: Adjunct publication*, 2014, pp. 1151–1160.

[12] A. B. McDonald and T. Znati, "A path availability model for wireless ad-hoc networks," in *WCNC. 1999 IEEE Wireless Communications and Networking Conference (Cat. No. 99TH8466)*, vol. 1. IEEE, 1999, pp. 35–40.

[13] G. Van Rossum and F. L. Drake, *Python 3 Reference Manual*. Scotts Valley, CA: CreateSpace, 2009.

[14] S. L. Brunton and J. N. Kutz, *Data-driven science and engineering: Machine learning, dynamical systems, and control*. Cambridge University Press, 2019.

[15] F. Pedregosa, G. Varoquaux, A. Gramfort, V. Michel, B. Thirion, O. Grisel, M. Blondel, P. Prettenhofer, R. Weiss, V. Dubourg, J. Vanderplas, A. Passos, D. Cournapeau, M. Brucher, M. Perrot, and E. Duchesnay, "Scikit-learn: Machine learning in Python," *Journal of Machine Learning Research*, vol. 12, pp. 2825–2830, 2011.

[16] K. J. Lakshminarasimhan, M. Petsalis, H. Park, G. C. DeAngelis, X. Pitkow, and D. E. Angelaki, "A dynamic bayesian observer model reveals origins of bias in visual path integration," *Neuron*, vol. 99, no. 1, pp. 194–206, 2018.

[17] E. Rovira, R. S. Mackie, N. Clark, P. N. Squire, M. D. Hendricks, A. M. Pulido, and P. M. Greenwood, "A role for attention during wilderness navigation: Comparing effects of bdnf, kibra, and chrna4." *Neuropsychology*, vol. 30, no. 6, p. 709, 2016.

[18] E. Vilar, F. Rebelo, and P. Noriega, "Indoor human wayfinding performance using vertical and horizontal signage in virtual reality," *Human Factors and Ergonomics in Manufacturing & Service Industries*, vol. 24, no. 6, pp. 601–615, 2014.

[19] A. J. Aretz and C. D. Wickens, "The mental rotation of map displays," *Human performance*, vol. 5, no. 4, pp. 303–328, 1992.

[20] R. Conroy, *Spatial navigation in immersive virtual environments*. University of London, University College London (United Kingdom), 2001.

[21] R. G. Golledge, "Path selection and route preference in human navigation: A progress report," in *International conference on spatial information theory*. Springer, 1995, pp. 207–222.

[22] K.-F. Richter and A. Klippel, "A model for context-specific route directions," in *International Conference on Spatial Cognition*. Springer, 2004, pp. 58–78.

[23] L. Bucher, F. Röser, J. Nejasmic, and K. Hamburger, "Belief revision and way-finding," *Cognitive processing*, vol. 15, no. 1, pp. 99–106, 2014.

[24] P. Jansen-Osmann and P. Fuchs, "Wayfinding behavior and spatial knowledge of adults and children in a virtual environment: The role of landmarks," *Experimental Psychology*, vol. 53,

no. 3, pp. 171–181, 2006.

[25] L. Korthauer, N. Nowak, M. Frahmand, and I. Driscoll, "Cognitive correlates of spatial navigation: associations between executive functioning and the virtual morris water task," *Behavioural brain research*, vol. 317, pp. 470–478, 2017.

[26] R. P. Darken and J. L. Sibert, "Navigating large virtual spaces," *International Journal of Human-Computer Interaction*, vol. 8, no. 1, pp. 49–71, 1996.

[27] F. T. Liu, K. M. Ting, and Z.-H. Zhou, "Isolation forest," in *2008 eighth ieee international conference on data mining*. IEEE, 2008, pp. 413–422.

[28] R. Johnston, K. Jones, and D. Manley, "Confounding and collinearity in regression analysis: a cautionary tale and an alternative procedure, illustrated by studies of british voting behaviour," *Quality & quantity*, vol. 52, no. 4, pp. 1957–1976, 2018.

[29] M. Schulz and K. Stattegger, "Spectrum: Spectral analysis of unevenly spaced paleoclimatic time series," *Computers & Geosciences*, vol. 23, no. 9, pp. 929–945, 1997.

[30] K. Rehfeld, N. Marwan, J. Heitzig, and J. Kurths, "Comparison of correlation analysis techniques for irregularly sampled time series," *Nonlinear Processes in Geophysics*, vol. 18, no. 3, pp. 389–404, 2011.

[31] J. Hort, J. Laczó, M. Vyhnálek, M. Bojar, J. Bureš, and K. Vlček, "Spatial navigation deficit in amnestic mild cognitive impairment," *Proceedings of the National Academy of Sciences*, vol. 104, no. 10, pp. 4042–4047, 2007.

[32] M. T. Schultheis, J. Himelstein, and A. A. Rizzo, "Virtual reality and neuropsychology: upgrading the current tools," *The Journal of head trauma rehabilitation*, vol. 17, no. 5, pp. 378–394, 2002.

[33] M. Rabuffetti, E. Farina, M. Alberoni, D. Pellegatta, I. Appollonio, P. Affanni, M. Forni, and M. Ferrarin, "Spatio-temporal features of visual exploration in unilaterally brain-damaged subjects with or without neglect: results from a touchscreen test," *PLoS one*, vol. 7, no. 2, p. e31511, 2012.

[34] A. Lamontagne, C. Paquette, and J. Fung, "Stroke affects the coordination of gaze and posture during preplanned turns while walking," *Neurorehabilitation and Neural Repair*, vol. 21, no. 1, pp. 62–67, 2007.

[35] M. Smithson and J. Verkuilen, "A better lemon squeezer? maximum-likelihood regression with beta-distributed dependent variables." *Psychological methods*, vol. 11, no. 1, p. 54, 2006.

[36] C. R. Oliveira, B. J. P. Lopes Filho, M. A. Sugarman, C. S. Esteves, M. M. B. Lima,

C. Moret-Tatay, T. Q. Irigaray, and I. I. L. Argimon, "Development and feasibility of a virtual reality task for the cognitive assessment of older adults: the eco-vr," *The Spanish journal of psychology*, vol. 19, 2016.

Appendices

A

	Measures				
	Number of occurrences	Mumber of occurrences per meter	Total duration of occurrences	Average duration of occurrences	**Number of features**
Movement properties					
Time	-	-	-	-	1
Distance	-	-	-	-	1
Average speed	-	-	-	-	1
wayfinding events					
Stopping behaviour	X	X	X	X	4
Slowing behaviour	X	X	X	X	4
Speeding behaviour	X	X	X	X	4
Direction changes	X	X			2
Straight walking behaviour	X	X	X	X	4
Smooth turns	X	X	X	X	4
Complex turns	X	X	X	X	4
Smooth continuations	X	X	X	X	4
Complex continuations	X	X	X	X	4
Path intersections	X	X			2

	Ailse types				
	Horizontal	Vertical	Target	Nontarget	
Movement properties					
Time	X	X	X	X	4
Distance	X	X	X	X	4
Average speed	X	X	X	X	4
wayfinding events					
Stopping behaviour	X	X	X	X	16
Slowing behaviour	X	X	X	X	16
Speeding behaviour	X	X	X	X	16
Direction changes	X	X	X	X	8
Straight walking behaviour	X	X	X	X	16
Smooth turns	X	X	X	X	16
Complex turns	X	X	X	X	16
Smooth continuations	X	X	X	X	16
Complex continuations	X	X	X	X	16
Path intersections	X	X	X	X	8
Revisits	X	X	X	X	4
				Total	199